



Sensitivity of Asian climate change to radiative forcing during the last millennium in a multi-model analysis



Zhengguo Shi^{a,b,c,*}, Tingting Xu^a, Hongli Wang^d

^a State Key Laboratory of Loess and Quaternary Geology, Institute of Earth Environment, Chinese Academy of Sciences, Xi'an 710061, China

^b Joint Center for Global Change Studies, Beijing 100875, China

^c CAS Center for Excellence in Tibetan Plateau Earth Sciences, Beijing 100101, China

^d Shaanxi Radio & TV University, Xi'an 710119, China

ARTICLE INFO

Article history:

Received 31 August 2015

Received in revised form 18 December 2015

Accepted 20 February 2016

Available online 26 February 2016

Keywords:

Asian climate

Last millennium

Climate sensitivity

Radiative forcing

Model intercomparison

ABSTRACT

The outputs of last millennium (A.D. 850–1850) experiments from seven climate models of the Paleoclimate Modeling Intercomparison Project 3, have been used to analyze decadal to centennial climatic variations over Asia, including the Indian monsoon, the East Asian monsoon and the westerly jet. In particular, the differences between the Medieval Warm Period (MWP, A.D. 901–1200) and the Little Ice Age (LIA, A.D. 1551–1850) are focused on. Statistically, significant temperature contrasts between the MWP and LIA are simulated by all of the models, and larger temperature deviations occur during colder periods. Although discrepancies exist, stronger Indian and East Asian summer monsoon circulations, as well as a stronger Asian westerly jet stream in winter, are found during the MWP compared to the LIA, in most of the models. These changes primarily originate from different atmospheric thermal structures over the two periods, which occur in response to the external radiative forcings. However, the monsoon-associated precipitation is quite complicated, with distinctly different patterns simulated among the models. There are phase differences in the multi-decadal variability of precipitation among the models, which consistently fail to detect a weakening in the precipitation at the minima of the radiative forcings. Only limited models are able to simulate the quasi-100-year solar cycles in the changes of precipitation over India and East Asia. Thus, although the climate system is certainly affected by external radiative forcings, our results imply that the natural forcings may not exert such a substantial influence on the Asian monsoon rainfall, or the models may underestimate the response.

© 2016 Elsevier B.V. All rights reserved.

1. Introduction

The Asian climate is characterized by a prominent coastal monsoon and inner aridity, and is an important component in the global climate system. The Asian monsoon, which includes the Indian and East Asian monsoons, provides fundamental water resources for the economic and social lives of a large proportion of the world's population. Over inland regions where the Asian monsoon hardly penetrates into, the precipitation is quite scarce and the westerly winds dominate nearly all year round.

The variation and evolution of the Asian monsoon and the westerly winds have basically controlled the patterns of climate change over Asia in modern- and paleo-times, and thus have attracted intensive studies (Gadgil, 2003; Ding and Chan, 2005; Wang, 2006; Zhang et al., 2006; Zhou et al., 2009; Lu et al., 2011; An et al., 2012, 2015; Shi et al., 2014). Among modern climate studies, the main focus has been on the variability of the Asian climate at relatively short timescales, from interseasonal to interdecadal, and their associated mechanisms, due to

the limited time coverage of observational data. Further, in most cases, researches based on modern observations have only analyzed the internal oscillations of the climate system (e.g., Kumar et al. (1999); Chang et al. (2001); Goswami and Xavier (2005); Goswami et al. (2006); Sun et al. (2008); Wang et al. (2008); Ummenhofer et al. (2011); Rajagopalan and Molnar (2012) and Xu et al. (2015)) and has failed to consider the various changes in external forcings.

The external forcing that has been considered the most till now is the variation of greenhouse gases (GHG); GHG forcing has been proven to exert a significant role on the Asian climate change. Not only does the GHG forcing directly affect the interdecadal variations of the Asian monsoon (Ueda et al., 2006; Li et al., 2010; Sooraj et al., 2014), but it might also be responsible for changes in the internal monsoon dynamics (Krishnamurti and Goswami, 2000; Wu and Wang, 2002; Wang et al., 2008). Other external forcings, for example, solar irradiation and volcanic activities, may also have significant impacts. However, our knowledge on the decadal to centennial variations of the Asian climate and mechanisms associated with them are still limited. How the external forcings, especially natural ones, affect the climate and internal dynamics over Asia remain largely unclear.

* Corresponding author at: State Key Laboratory of Loess and Quaternary Geology, Institute of Earth Environment, Chinese Academy of Sciences, Xi'an 710061, China.

The last millennium is a good period to explore the decadal to centennial variations in the Asian climate. For this period, the climate variability over Asia has basically been reconstructed from various geological proxies, including tree rings, stalagmites, corals and lake deposits. Remarkable fluctuations have been shown in the proxy data, for both the Indian and East Asian monsoon regions, on the decadal to centennial time scales (e.g., Qian et al. (2003); Zheng et al. (2006); Zhang et al. (2008); Cook et al. (2010); Berkelhammer et al. (2010) and Sinha et al. (2011), 2015). In particular, severe droughts occurred in India and eastern China during solar minima, which indicates that the monsoons were simultaneously weakened during these periods (Agnihotri et al., 2002). However, reconstruction data from eastern Africa has shown the opposite behavior in that region (Verschuren et al., 2000). Nevertheless, from these data reconstructions, it is clear that some changes in the monsoons can be explained by manifestations of solar variability.

Two typical periods of the last millennium, the Medieval Warm Period (MWP) and the Little Ice Age (LIA), are documented within the climate proxies over Asia; in most proxies, distinct differences can be seen between the two periods. In large parts of northern China, warmer and wetter MWP climate anomalies can be seen in the proxies (Zhang et al., 2008). In southern China, these differences are not as distinct (Wang et al., 2005) and in certain areas, it appears that more precipitation occurred during the LIA (Zheng et al., 2006). Some proxies from India (von Rad et al., 1999; Sinha et al., 2007) indicate that the MWP was relatively wetter, while the driest period in the last millennium occurred during the transition into the early stages of the LIA. In addition, an apparently stronger upwelling occurred during the MWP in the Arabian Sea (Anderson et al., 2002), which might support an intensified Indian monsoon. In contrast, precipitation during the MWP decreased across the arid regions, from coastal Arabia to inland central Asia (Chen et al., 2008, 2010).

Although there have been intensive researches, through reconstructions, into Asian climate change over the past millennium, the proxy records used originated from specific sites, and so are unable to provide detailed climatological fields; thus, in this context, numerical experiments that cover the period provide a good supplementary tool, to explore the mechanisms of climate change. Using reconstructions of the boundary conditions, lots of climate models have been forced to simulate climate change over the past millennium, however, most of the studies have focused on global or hemispheric temperatures (e.g., Brovkin et al. (1999); Bertrand et al. (2002); Zorita et al. (2004); Goosse et al. (2005); Ammann et al. (2007) and Shi et al. (2007)). In terms of the Asian climate, most researches have concentrated on the long-term variability of the Asian monsoon, and in particular, precipitation over East Asia (Shen et al., 2008; Liu et al., 2011; Man et al., 2012).

Through analysis of the millennium model simulations, a significant centennial oscillation has been detected in the summer precipitation over eastern China, which is essentially a forced response, linked to the fluctuations of insolation and volcanic aerosols (Chen et al., 2008; Liu et al., 2011; Man et al., 2012). The response of the East Asian summer monsoon to external forcings, measured by the differences between the MWP and LIA, is also remarkable (Liu et al., 2011; Man et al., 2012). In addition, the spatial patterns observed are different from the interannual variability (Liu et al., 2011). Further, it has been found that the strength of the response may be latitude-dependent and precipitation over different latitudinal belts is sensitive to different forcings (Liu et al., 2011). Internally, ocean feedback also plays a role, and changes in the sea surface temperatures over the Pacific are of importance, in explaining the long-term variation of the Asian monsoon (Fan et al., 2009; Graham et al., 2011).

All the previous modeling studies have indicated that Asian climate change during the past millennium is a forced response, and that the response is significant; however, it is unknown whether the results of these studies are model-dependent. Thus, a multi-model analysis is conducted here, to examine the sensitivity of different models to the

Table 1

List of models used for the last millennium experiments in this study.

Model	Atmospheric resolution	Ensemble
CCSM4	288 × 192 × L26	r1i1p1
HadCM3	96 × 73 × L19	r1i1p1
BCC-CSM1-1	128 × 64 × L26	r1i1p1
CSIRO-Mk3L-1-2	64 × 56 × L18	r1i1p1
MPI-ESM-P	196 × 98 × L47	r1i1p1
GISS-E2-R	144 × 90 × L40	r1i1p124
IPSL-CM5A-LR	96 × 95 × L39	r1i1p1

external forcings, during the last millennium. The main aims of this study are to identify: (1) how the Asian climate responds to external radiative forcings on the decadal to centennial timescale; (2) whether the remarkable temperature difference between the MWP and LIA could induce any differences in the Asian climate; (3) what the consistencies are among the modeling results and what the differences are. To answer these questions, the multi-decadal to centennial variability of Asian climate and its relation with the radiative forcing, as well as the differences between the MWP and LIA, are calculated and analyzed for all seven models. A short description of the last millennium experiments is presented in Section 2. The results are analyzed and discussed in Sections 3 and 4, respectively, and Section 5 provides a summary of this study.

2. Last millennium experiments

The modeling data used in this study are from the last millennium (LM) and the preindustrial control experiments, produced by seven different climate models. The data are available from the Paleoclimate Modeling Intercomparison Project 3 (PMIP3) and can be downloaded at the Earth System Grid Federation. All the models are coupled ocean–atmosphere models performed at various resolutions (Table 1). These models are integrated across the period A.D. 850–1850; so the models allow us to test the sensitivity of climate systems during the pre-industrial era. The simulations are performed with similar external forcings (Fig. 1), including solar irradiation, volcanic aerosols, land cover changes and greenhouse gases. The forcings used are discussed in detail by Schmidt et al. (2012), who demonstrate that, in general, there is similar variation in the forcings among the simulations. We note that all the experiments have used SBF and VSK reconstructions for solar changes (Steinhilber et al., 2009; Vieira et al., 2011); these data indicate that the solar irradiation varied by a range of 0.3 W/m² during the past millennium, which is a much smaller range than indicated by the SEA data (Shapiro et al., 2011). In addition, the radiative forcing of volcanic aerosols is larger, by about 9 and 7 W/m² for the 1250s and 1450s eruptions, respectively, in Indonesia and Vanuatu, in GRA data, than in CEA data

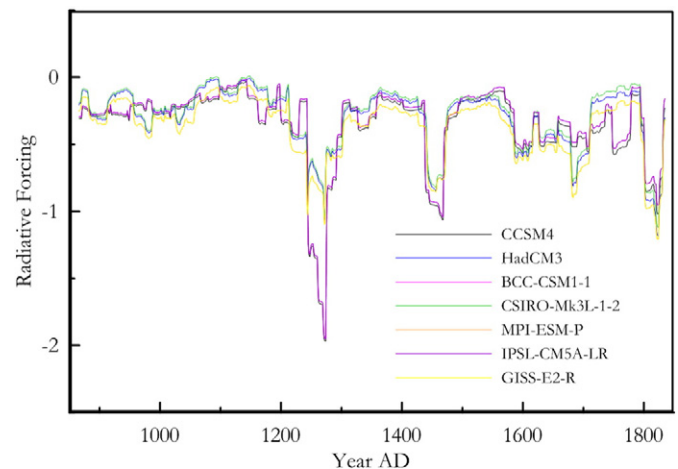


Fig. 1. Radiative forcings (W/m²) used for the seven last millennium experiments. The curves are 31 year smoothed.

(Crowley et al., 2008; Gao et al., 2008); the larger GRA forcing is used in the BCC-CSM1-1, IPSL-CM5A-LR and CCSM4 experiments. Detailed descriptions on the models and the experimental design can be found on the PMIP3 websites.

The model performances of the Asian climate have been validated by comparing the surface temperature and precipitation data (Fig. 2). Although the spatial resolution varies among the models, the basic patterns of the simulated temperatures and precipitation rates are in good agreement with observations (Fig. 2). The surface temperatures generally decrease from the tropics to the high-latitudes, with the exception of the Tibetan Plateau, where the high-altitude cooling

simulated by the models is stronger than that observed in the Climate Research Unit (CRU) data set. The pattern correlation coefficients between the CRU temperature and the different models vary from 0.99–0.98. In terms of precipitation, heavy rainfall occurs over the tropical oceans and Asian monsoon regions, and light rainfall occurs over inland Asia. The rain belts across the southern slopes of the Himalayas are simulated in CCSM4 and MPI-ESM-P, due to the high resolutions; this pattern is not seen in the observational data. The simulated precipitation in IPSL-CM5A-LR is partly underestimated over the monsoon areas. The pattern correlation coefficients of the precipitation data vary from 0.88–0.68, with the lowest (0.68) between the observational data and

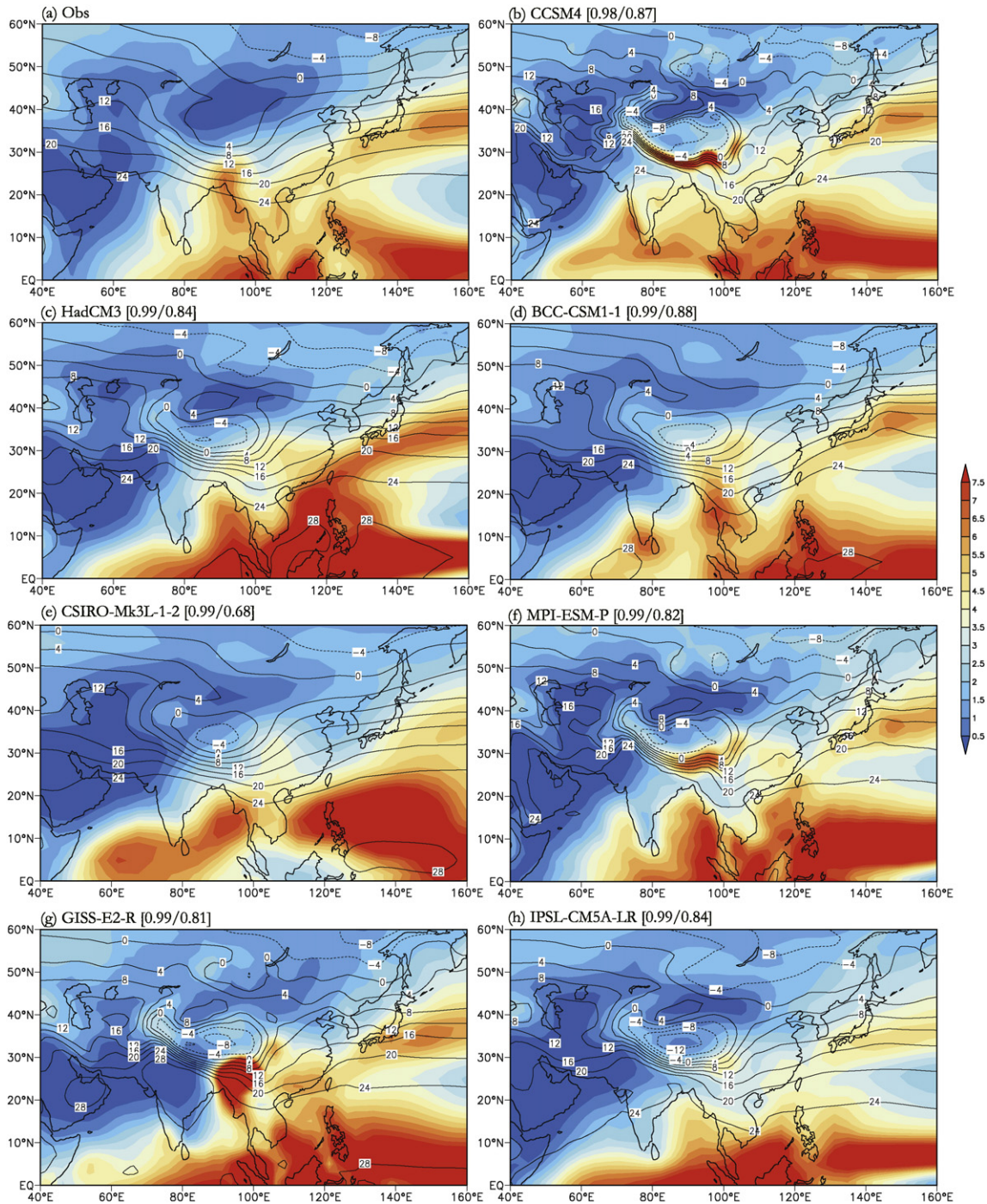


Fig. 2. Comparisons of the climatological annual mean surface temperatures ($^{\circ}\text{C}$, contour) and precipitation rates (mm/d, shaded) over Asia. (a) Observed temperatures and precipitation rates from the CRU and GPCP data sets, respectively; (b–h) Results simulated by the seven models in the pre-industrial experiments. The spatial correlations between the observations and simulations of the temperatures and precipitation rates are shown in the brackets.

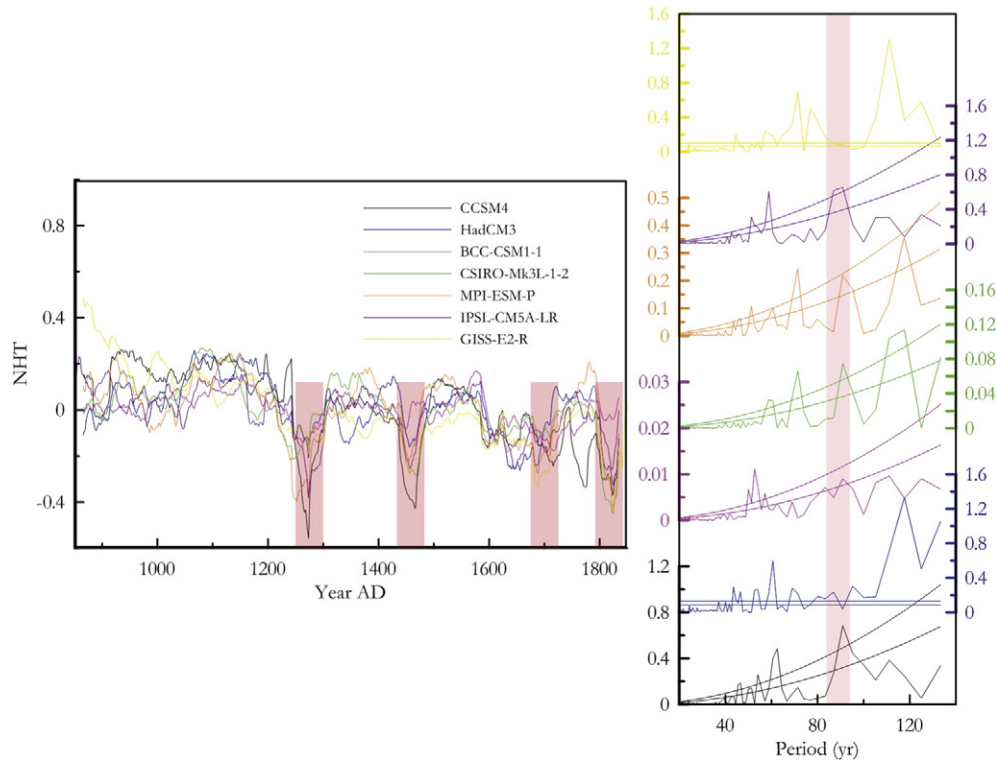


Fig. 3. Simulated 31-year averaged northern hemisphere surface temperature anomalies ($^{\circ}\text{C}$, left panel) and their periods (year, right panel) during the past millennium. The anomalies are calculated based on the mean values of the whole period. Pink shading indicates the periods of minimal radiative forcings and the 88 year solar cycles in the left and right panels, respectively. T-test curves used for the 95% and 99% confidence levels are also shown for reference.

the CSIRO-Mk3L-1-2 simulation. In summary, although small biases exist, the spatial distributions of Asian surface temperatures and precipitation rates are simulated well by all of the models. This provides confidence, for the further analysis of variations in the climate over last millennium, using the model simulation outputs.

3. Results

3.1. Surface temperature

In general, all of the models have simulated remarkable multi-decadal to centennial responses in the northern hemisphere (NH) surface temperatures (Fig. 3). The two typical periods, the MWP and LIA, are also detected in the simulations, around the years A.D. 901–1200 and 1551–1850, respectively. Significant differences between the MWP and LIA are found in all of the models, with annual mean values ranging from $0.08\text{ }^{\circ}\text{C}$ – $0.30\text{ }^{\circ}\text{C}$ (Table 2); these changes are primarily explained by the different levels of radiative forcing during the two periods (0.21 – 0.24 W/m^2). Seasonally, the responses of temperature in summer are weaker ($0.05\text{ }^{\circ}\text{C}$ – $0.25\text{ }^{\circ}\text{C}$) than in winter ($0.12\text{ }^{\circ}\text{C}$ – $0.36\text{ }^{\circ}\text{C}$).

The multi-decadal variations in the NH temperatures follow changes in the radiative forcing well, with correlation coefficients of 0.55 – 0.90 (Table 3), which indicates that the radiative forcing is the dominated forcing for the NH temperatures. The NH consistently becomes cooler

Table 2
Differences in the northern hemisphere surface temperatures ($^{\circ}\text{C}$) between the Medieval Warm Period and Little Ice Age. ** indicates that the differences are statistically significant at the 99% level.

	CCSM	HadCM	BCC	CSIRO	MPI	GISS	IPSL
Annual	0.30**	0.20**	0.08**	0.18**	0.18**	0.26**	0.11**
JJA	0.25**	0.15**	0.06**	0.14**	0.13**	0.21**	0.05**
DJF	0.36**	0.23**	0.12**	0.21**	0.22**	0.30**	0.14**

in the simulations during radiation minima, under the impact of both solar and volcanic activities; however, the amplitudes of change differ among the models, due to the different forcings and model sensitivities. Among the seven models, the CCSM4 simulated response is the most significant.

Power spectrum analysis of the temperature data shows strong quasi-100-year cycles in temperatures for the IPSL-CM5A-LR, MPI-ESM-P, CSIRO-Mk3L-1-2, BCC-CSM1-1 and CCSM4 simulations, in good agreement with the 88 year solar cycle (Gleissberg cycle). This highlights the influence of solar cycle in modulating the temperatures at this timescale (Fig. 4). In addition, there are significant changes in temperatures over shorter periods, of 40–60 yr, in the models; these might be associated with the internal dynamics in the climate system, especially with the changes in sea surface temperatures in the Pacific and Atlantic (e.g., Atlantic Multi-decadal Oscillation and Pacific Decadal Oscillation). In HadCM3 and GISS-E2-R, no clear solar cycles are detected in the NH temperature although their long-term temperature trends share significant correlations with the radiative forcing (Table 3). The maxima in the standard deviations usually occur during the coldest periods simulated by the models (Fig. 4), indicating that the interannual fluctuations of the NH temperatures are intensified at the radiation

Table 3
Correlation coefficients between the northern hemisphere temperature and Asian precipitation, with radiative forcing. **/* indicates statistically significant at 99%/95% levels, respectively.

	CCSM	HadCM	BCC	CSIRO	MPI	GISS	IPSL
NH SAT	0.77**	0.74**	0.55**	0.81**	0.90**	0.66**	0.71**
South Asian Pr	0.62**	−0.07	−0.05	0.47**	0.43**	0.36**	−0.21**
East Asian Pr	0.38**	0.41**	0.17	0.12	−0.14	0.28*	0.24**
Central Asian Pr	0.38**	0.16**	0.29*	−0.14	0.02	0.48**	0.48**

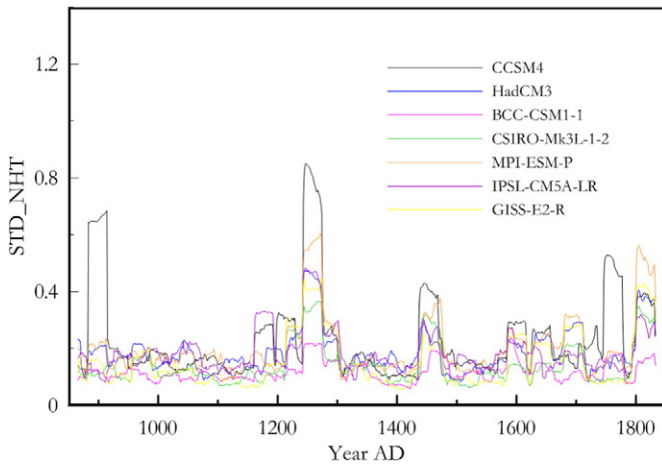


Fig. 4. Changes in the standard deviation of the northern hemisphere surface temperatures, calculated using a 31 year window.

minima. The only exception is in the CCSM4 simulation in which the standard deviation is quite large around A.D. 900, even though the simulated cooling is not that remarkable (Fig. 4).

Spatially, the larger radiative forcing during the MWP warms the NH continents and oceans more in summer over Asia, compared to that during the LIA (Fig. 5). In five of the seven models, the JJA temperature differences between the MWP and LIA are statistically significant, over the broad areas across Asia and the adjacent oceans; in contrast however, the changes simulated in the BCC-CSM1-1 and IPSL-CM5A-LR experiments are quite limited or insignificant. The simulated temperature changes are about 0.2 °C, or more, over continental Asia, in CCSM4 and GISS-E2-R experiments; this warming of the land is largest over the arid areas. Due to different thermal inertia, the surface temperature changes over the ocean are usually smaller than those over the land. This pattern of warmer lands and less warm oceans allows a strengthened ocean–land thermal contrast. Negative anomalies between the MWP and LIA are found over certain regions of the Indian subcontinent and Indian Ocean in most model simulations, although they are not remarkable.

In December–January–February (DJF), the MWP surface temperatures are higher than those in the LIA, however, the locations of the anomalies differ (Fig. 6). The simulated temperature differences are usually statistically significant over the oceans, but not over large continental areas. A consistent warming center occurs over the Sea of Okhotsk in all of the model simulations, by 0.4 °C or more, except in the MPI-ESM-P and IPSL-CM5A-LR ones. Another center detected by the HadCM3, BCC-CSM1-1 and MPI-ESM-P models is located in the mid-latitude, inland regions, where the MWP warming is also obvious in JJA; this indicates that the arid/semi-arid areas might be sensitive to radiative forcing.

3.2. Circulation

Response of the low-level Asian summer and winter monsoon and high-level westerly circulations is analyzed here. The differences in the JJA 850 hPa wind vectors, between the MWP and LIA, in the seven models are shown in Fig. 7. In CCSM4, obvious and statistically significant westerly wind anomalies are simulated over southern and southeastern Asia in summer (Fig. 7a). This indicates that the Indian monsoon is stronger during the MWP compared to the LIA. Over East Asia, the intensified southerly winds in the northern region enhance the movement of water vapor from the ocean to the continent. Similar with CCSM4, the simulated Indian and East Asian monsoons, by the HadCM3, CSIRO-Mk3L-1-2, MPI-ESM-P and GISS-E2-R experiments, are also intensified during the MWP, characterized by anomalous westerly and southerly winds, respectively (Fig. 7b, d–f). The responses of

the Asian monsoon circulation are closely associated with the strengthened ocean–land thermal contrasts (Fig. 5). Over the 200 hPa isobaric surface, the Bonin high simulated in most models is significantly intensified during the MWP (Fig. 8), which contributes to the clockwise circulation anomalies over northern East Asia (Fig. 7a, d–f). In addition, the simulated Tibetan high is also strengthened, although this is not as evident as the Bonin high.

In contrast to the summer monsoon, the differences in East Asian winter monsoon, between the MWP and LIA simulated by the models are quite inconsistent (Fig. 9). Statistically significant southerly wind anomalies over the East Asian regions are detected by three of the models (CCSM4, HadCM3 and GISS-E2-R), indicating that the East Asian winter monsoon is weaker during the MWP. In contrast, anomalous northerly winds are simulated by the other four models, which does not support the traditional viewpoint that the winter monsoon is usually stronger during colder periods. Although the changes in winter precipitation are not very remarkable, we can still see that weaker winter monsoon winds are accompanied by wetter conditions over most parts of East Asia during the MWP, but stronger winter monsoon winds can induce drier conditions (Fig. 9). In south Asia, the winter monsoon circulations are intensified during the MWP according to the CSIRO-Mk3L-1-2, MPI-ESM-P, GISS-E2-R and IPSL-CM5A-LR models (Fig. 9d–g), and no model simulates a weaker Indian winter monsoon during the MWP compared to the LIA.

In the upper atmosphere, the westerly winds dominate at the mid-latitudes (about 40°N) and a maximum center of the westerly jet stream emerges across central Asia to Japan. The differences in the mid-latitude westerly winds over Asia in winter between the MWP and LIA, in the seven models are mostly obvious (Fig. 10). In the zonal belt of 30–50°N, the westerly wind velocities during the MWP are significantly larger than during the LIA in five of the model simulations (HadCM3, CSIRO-Mk3L-1-2, MPI-ESM-P, GISS-E2-R and IPSL-CM5A-LR). The increases during the MWP are different in their magnitude, with the largest being produced by the MPI-ESM-P simulation, consisting of a maximum center of approximately 1.6 m/s over northern China. Over the westerly jet region, the simulated wind speeds are consistently higher during the MWP, which indicates that the Asian jet tends to be strengthened during warm periods. However, the changes in the westerly winds are not remarkable in either of the CCSM4 and BCC-CSM1-1 simulations and the differences between the MWP and LIA are rarely statistically significant over the whole of Asia. The changes in the thermal structure in the middle to high levels vary similarly among the different models (Fig. 11). Over the extratropical regions, the atmospheric warming during the MWP gradually decreases from the lower to the higher latitudes and in some model simulations (MPI-ESM-P, GISS-E2-R and IPSL-CM5A-LR) the positive temperature anomalies are reversed, to be negative, over Japan and the Sea of Okhotsk. The uneven temperature changes result in an intensified meridional thermal gradient, which facilitates the intensification of the westerly jet over Asia (Fig. 10).

3.3. Precipitation rate

The changes in precipitation over Asia at the multi-decadal to centennial timescale, simulated by the LM experiments, are examined in three climate zones: the Indian monsoon region (70–100°E, 10–25°N), the East Asian monsoon region (105–120°E, 25–45°N) and the inland arid region (60–90°E, 40–50°N). The anomalies of the averaged June–July–August (JJA) precipitation rates over the Indian monsoon region, simulated by the seven models, and their periods are shown in Fig. 12. All models have consistently simulated strong fluctuations on the multi-decadal to centennial scales in the south Asian rainfall, although the amplitudes vary. In the IPSL-CM5A-LR and MPI-ESM-P experiments, the changes in precipitation are restricted to a range of approximately 0.4 mm/d during the last millennium but the range increases to 0.8 mm/d in the CCSM4 experiment. Among the models, it is difficult

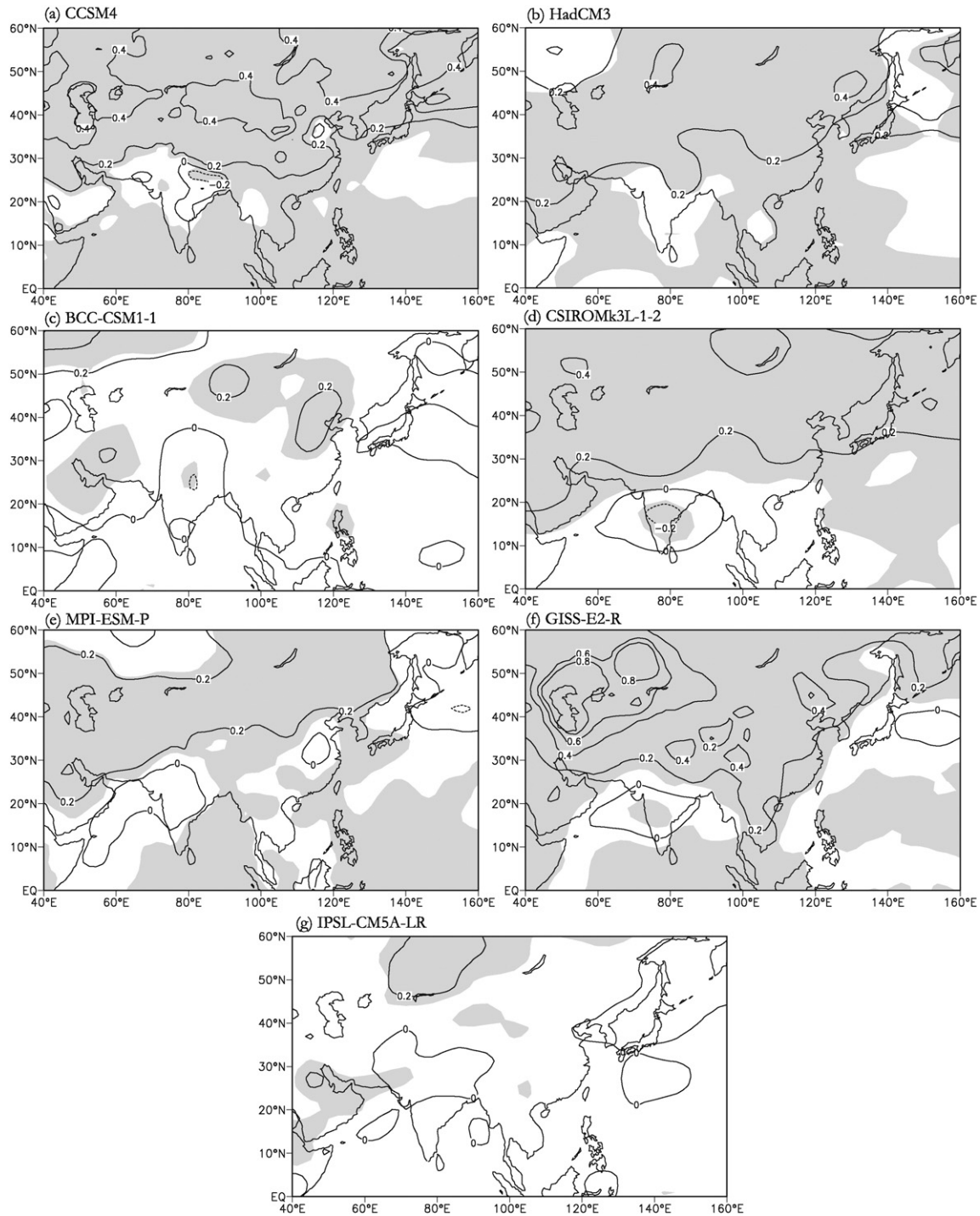


Fig. 5. Differences in the JJA surface temperatures over Asia between the MWP and the LIA. Shaded areas show the regions that are statistically significant at the 95% confidence level.

to detect similar changes in phase, to the contrary, the phase responses in the different models differ distinctly, and are even opposite during some time periods. The multi-decadal variability in precipitation is the most intense, with the main periods being 40–60 years long for the MPI-ESM-P and HadCM3 experiments, and 60–80 years for the GISS-E2-R, IPSL-CM5A-LR and BCC-CSM1-1 experiments; both phases of variation are seen in the CCSM4 simulation (Fig. 12). However, the solar cycles are missed in all seven models, which implies that changes in precipitation simulated by the models are not forced by the changes in solar irradiation.

The correlation coefficients between the south Asian precipitation rates and radiative forcing are much smaller than those for surface

temperature (Table 3); the best is found with the CCSM4 simulation (0.62). In other models, although the correlation coefficients are even less than 0.62, some of them are still statistically significant. In the IPSL simulation, the correlation is negative (-0.21). Despite the temperature differences between the MWP and LIA, the corresponding differences in the south Asian precipitation are not very evident for most models (Table 4), which indicates that the temperature differences do not lead to remarkable changes in precipitation. Only two models (CCSM4 and CSIRO-Mk3L-1-2) simulated significant positive anomalies, that is, the JJA precipitation is larger during the warmer MWP. At the four radiation minima, the precipitation simulated by CCSM4 is consistently at its lowest levels; however, this agreement does not occur in the

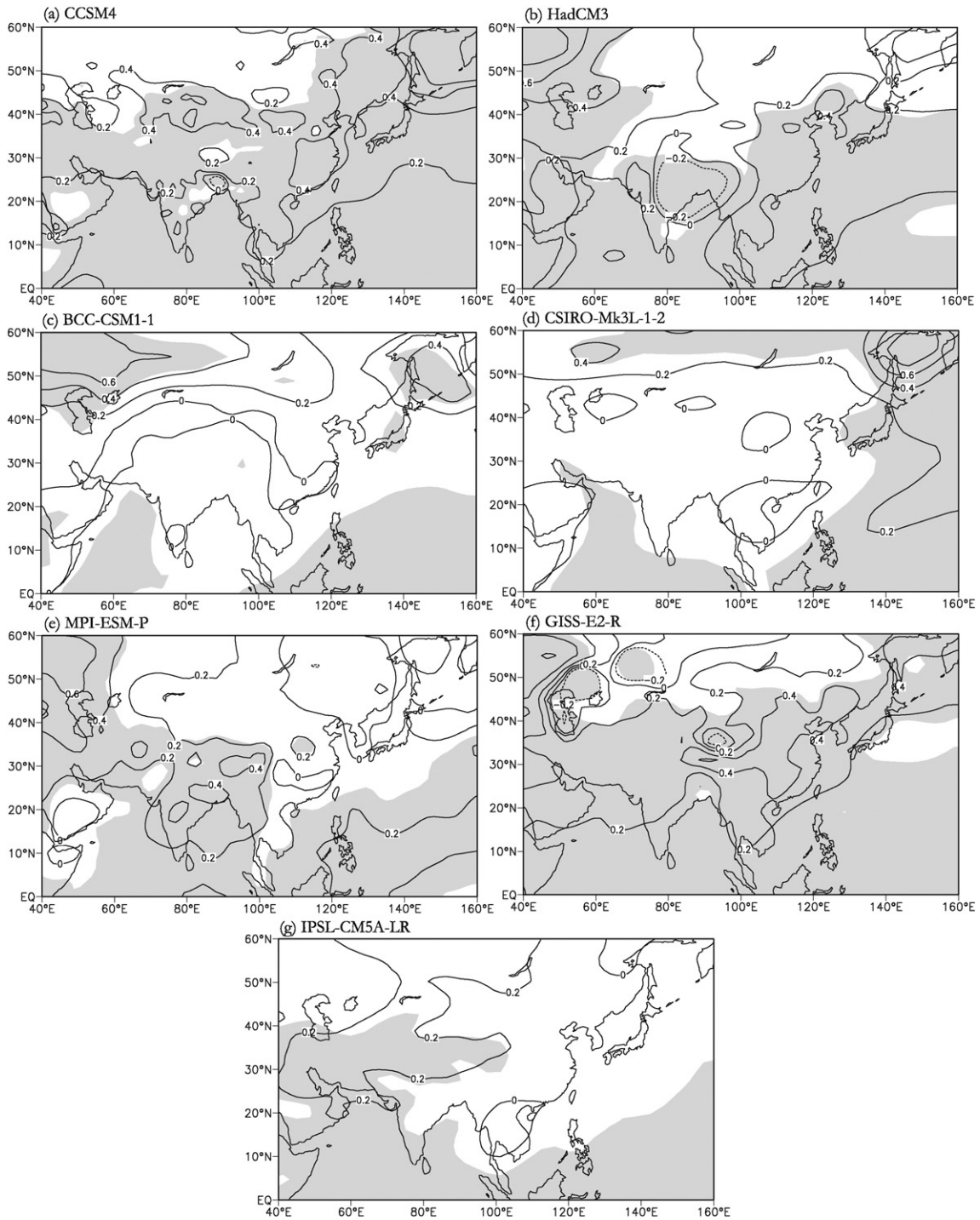


Fig. 6. Differences in the DJF surface temperatures over Asia between the MWP and LIA. Shaded areas show the regions that are statistically significant at 95% confidence level.

other models. In particular, some of the radiation minima correspond to peaks in precipitation levels in the BCC-ESM1-1 and HadCM3 experiments (Fig. 12). This implies that cooler conditions do not always lead to the suppression of rainfall. In summary, few models simulate a sensitive response of the south Asian JJA precipitation to the variations in radiative forcings during the last millennium.

In East Asia, multi-decadal variations in JJA precipitation rates are also simulated by all of the models, with amplitudes of 0.4 mm/d (Fig. 13). Some models (e.g., CCSM4 and CSIRO-Mk3L-1-2) simulate changes in the East Asian precipitation that are smaller than those simulated in the south Asian precipitation (Fig. 12). The phase responses of precipitation are distinctly different among the models,

so that consistent results are hardly ever found in any two models. It is also difficult to present an in-phase or out-of-phase relationship between the variations in the East and south Asian precipitation rates. This complexity of phase responses indicates that there are strong model dependencies in the simulated Asian monsoon rainfall.

The periods of East Asian precipitation occur on 60–80 year cycles, at a 99% confidence level, in most models (CCSM4, BCC-CSM1-1, IPSL-CM5A-LR and GISS-E2-R). Notably, the primary cycle that occurs in the HadCM3 simulation is ~87 years, in good agreement with the Gleissberg solar cycle, supporting the potential role of solar irradiation on the changes in precipitation. However, the correlations between the East Asian precipitation rates and radiative forcing are either

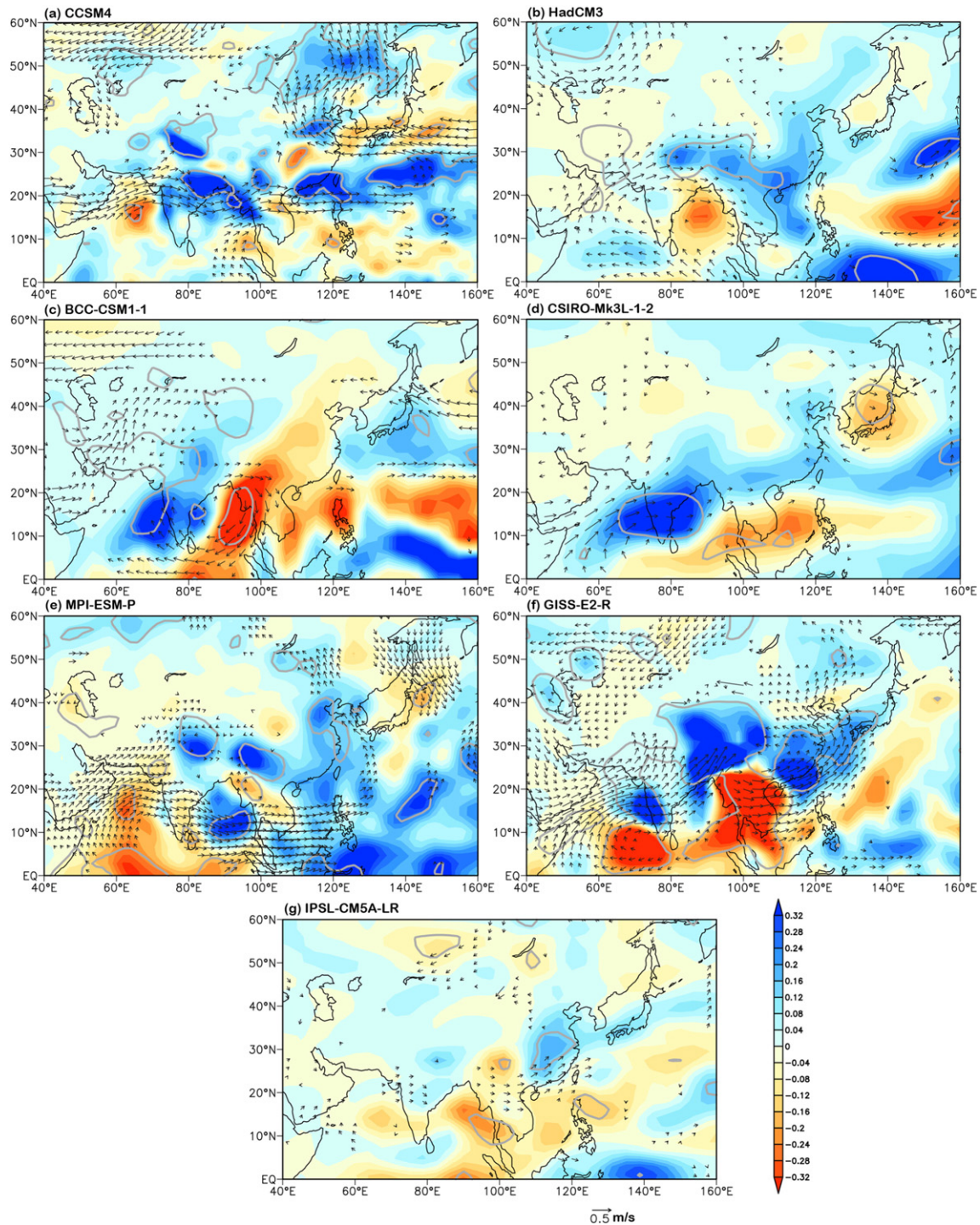


Fig. 7. Differences in the JJA 850 hPa wind vectors (m/s) and precipitation rates (mm/d) between the MWP and LIA. Regions that are statistically significant at 95% confidence level for the wind vectors and precipitation rates are shown as black and in the gray lines, respectively.

relatively weak or not significant at all (Table 3). The largest coefficients are approximately 0.4, simulated by the CCSM4 and HadCM3 experiments. The differences in precipitation between the MWP and LIA are statistically significant in four models, being about 0.1 mm/d (Table 4). At the radiation minima, the precipitation levels simulated in East Asia are not always at their lowest (Fig. 13), similar to that found for the south Asia (Fig. 12).

Spatially, the differences in precipitation between the MWP and LIA in CCSM4 are positive over most of the monsoon regions, including India, the Bay of Bengal, southeastern China and northern China (Fig. 7a). Three models (BCC-CSM1-1, CSIRO-Mk3L-1-2 and GISS-E2-

R) simulated an increase in precipitation over the Indian Peninsula and a decrease in precipitation over southeastern Asia, but the HadCM3 experiment modeled an increase in precipitation over southeastern Asia (Fig. 7b–d, f). Larger MWP precipitation levels occur over most parts of East Asia, including eastern China and the adjacent seas in HadCM3, CSIRO-Mk3L-1-2, MPI-ESM-P, GISS-E2-R and IPSL-CM5A-LR simulations. The exception is in the BCC-CSM1-1 simulation, which shows a negative difference between the MWP and the LIA; however, this difference is not significant. Japan is consistently found to be drier during the MWP, by the CCSM4, CSIRO-Mk3L-1-2 and MPI-ESM-P models, which is closely linked with the simulated anti-cyclone

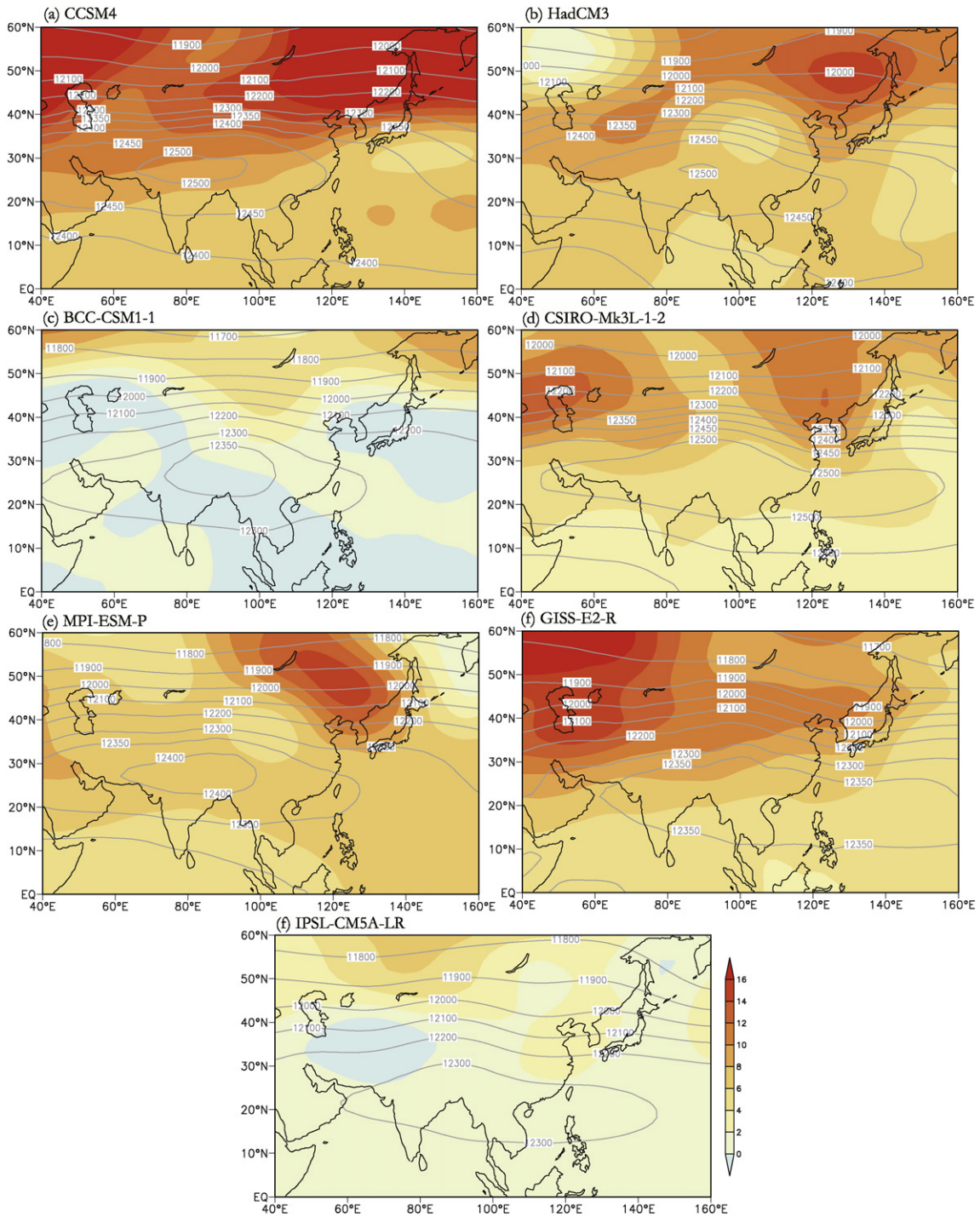


Fig. 8. JJA 200 hPa geopotential heights during the MWP, and their difference from those during the LIA.

anomalies over this region (Fig. 7). In brief, the spatial pattern of the precipitation response is quite complicated especially over low-latitude regions, although most of the models have simulated stronger Indian and East Asian monsoon circulations.

Changes in the annual precipitation rates over the arid region in central Asia, simulated by the seven models, are small over the past millennium (Fig. 14). In the CCSM4, BCC-CSM1-1 and CSIRO-Mk3L-1-2 simulations, the precipitation levels are periodical, with peaks every 60–80 years, similar with those over East and south Asian areas; however, no significant cycles are simulated in the other four models at the 99% confidence level. The MWP–LIA simulated differences are quite

limited, and in most cases they are not statistically significant (Figs. 7, 9). The 99% confidence anomalies in the CSIRO-Mk3L-1-2 simulation are negative, which indicates that the central Asian rainfall during the MWP might be weaker than during the LIA.

In order to further examine the precipitation responses to radiative forcing, the variations in precipitation in LM and preindustrial experiments by CCSM4, one with external forcing and the other without, are compared (Fig. 15). The NH temperatures are nearly unchanged over time, in the simulation without the radiative forcing. No solar cycle is detected and significant cyclical periods of about 60–70 years are actually associated with the internal oscillations of the climate system.

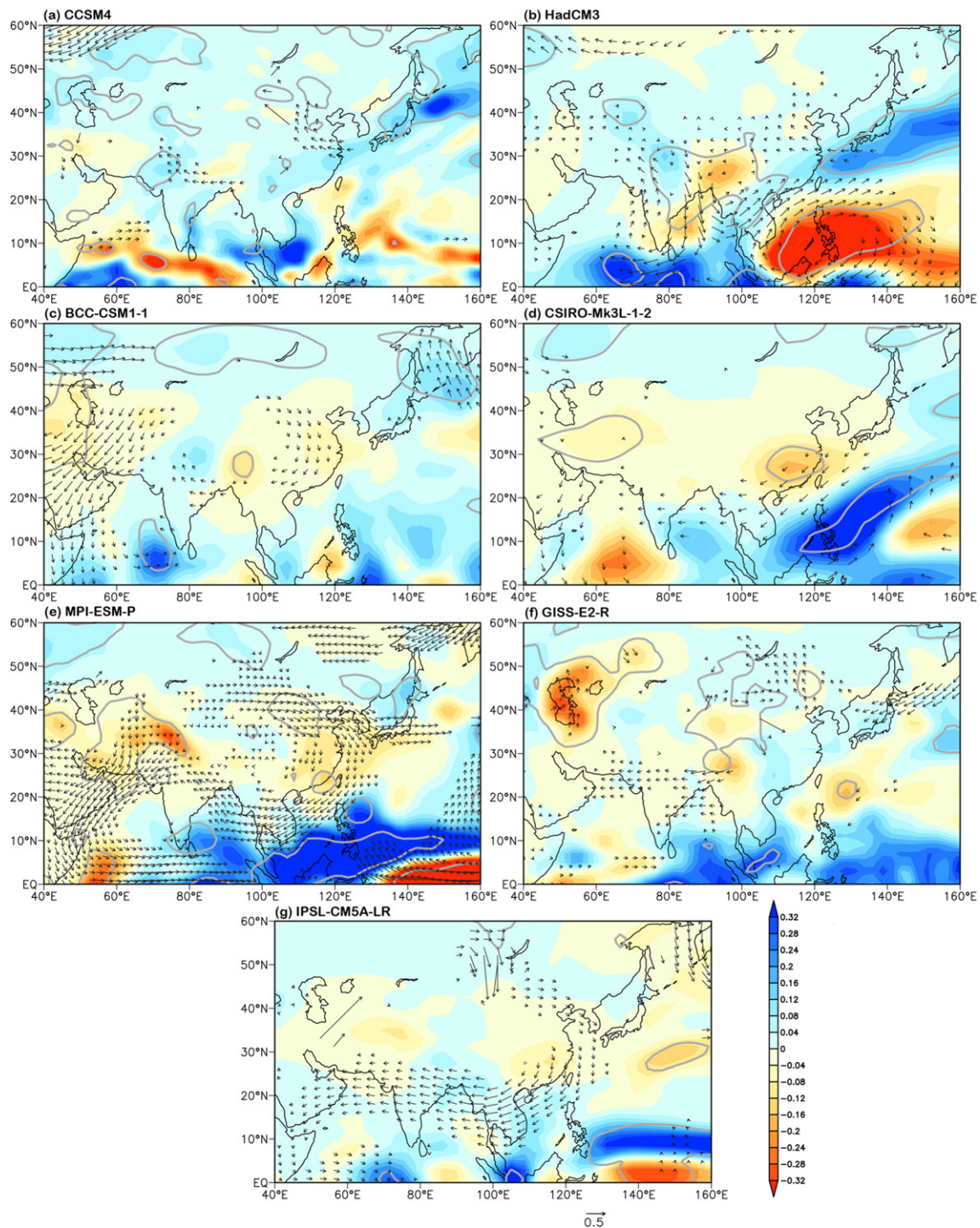


Fig. 9. Differences in the DJF 850 hPa wind vectors (m/s) and precipitation rates (mm/d) between the MWP and LIA. Regions that are statistically significant at 95% confidence level for the wind vectors and precipitation are shown as black and in the gray lines, respectively.

Further, the responses of the NH temperatures to the internal oscillations are much smaller than those to the external radiative forcing (Fig. 15). This remarkable effect of radiative forcing on temperature is not seen in the precipitation rates over all three of the climatic zones in Asia. The amplitudes of precipitation variation in the experiment without radiative forcing are similar to those in the forcing experiment with radiative forcing, and their periods are also restricted to 40–80 years (Fig. 15); this supports the notion that the variations in precipitation during the last millennium are primarily controlled by internal dynamics, and the role of external radiative forcing is limited.

4. Discussion

4.1. Model-data intercomparison

In order to compare the simulated and reconstructed climates over Asia, we chose several proxy data, mainly derived from historical documents, tree rings, stalagmites and lake deposits, which reflects the climatic variation during the last millennium. As the reconstructed temperature data indicate, the MWP and LIA stages existed over East Asian continent; they shared similar features with the whole of the NH, in that the warmer period during medieval times ended during

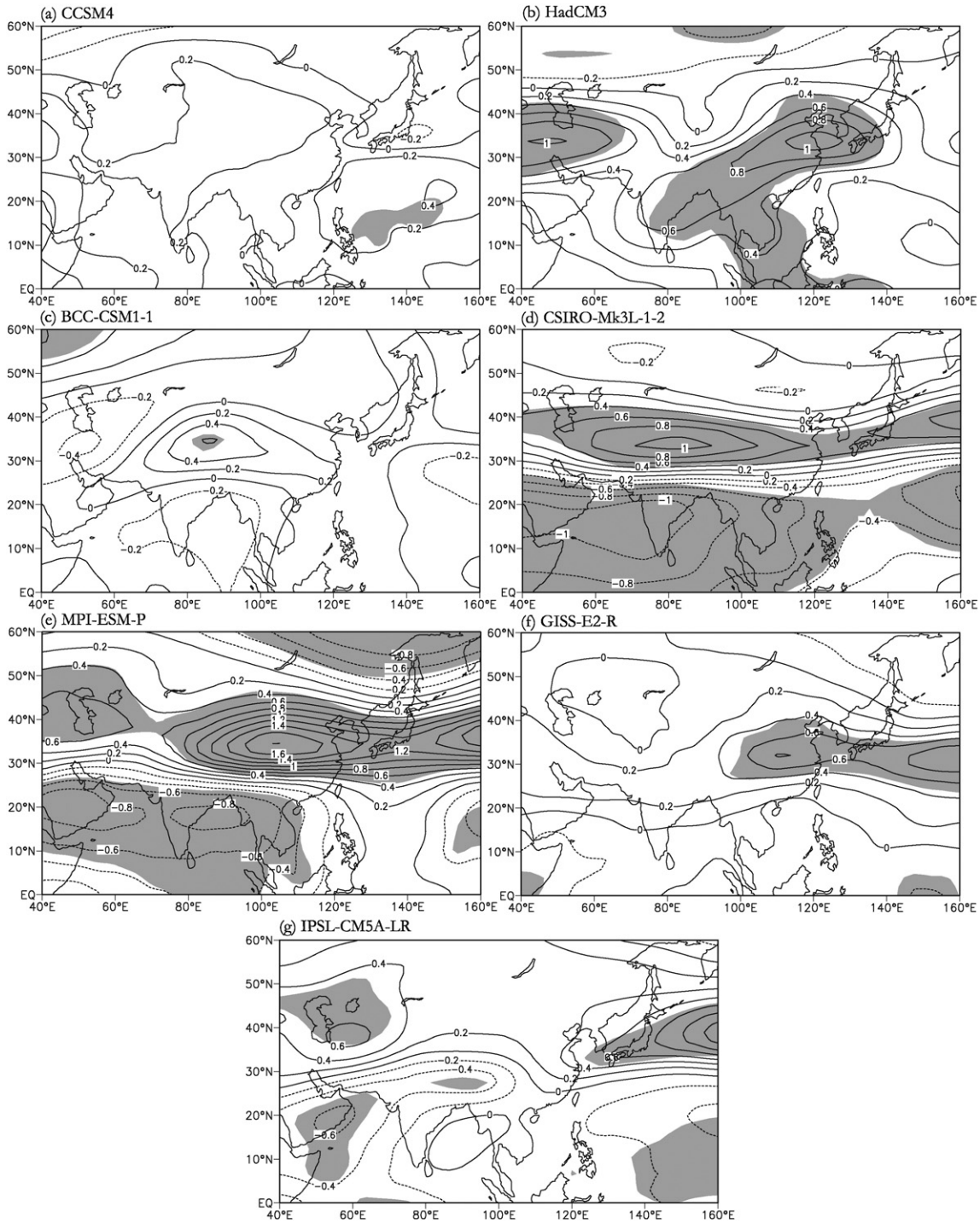


Fig. 10. Differences in the DJF 200 hPa zonal winds (m/s), between the MWP and LIA. Shaded areas show the regions that are statistically significant at the 95% confidence level.

the 12th century and the colder period was present from the 15th to the 19th centuries (Yang et al., 2002; Wang et al., 2007). The temperatures over the western tropical Pacific also present an obvious long-term cooling trend from the MWP to the LIA (Newton et al., 2006). The model simulations also show temperature differences between the two periods and positive anomalies occur over nearly the whole of the Asian region in both summer and winter, although in some simulations the differences are not significant. Overall, both the models and reconstructed data support the notion of temperature variation at the centennial-scale over Asia, during the last millennium.

Due to the various responses of the multi-decadal fluctuations in the Asian precipitation rates that occur in both the reconstructions

and simulations, it is difficult to check the model-data consistency in this respect. Therefore, we focus here on the differences between MWP and LIA. Among the seven models in the ensemble, two simulated a significant increase in the south Asian precipitation during the MWP, compared to the LIA, while the other models showed quite a limited response. Although the differences are not spatially homogeneous, most of simulations present greater levels of precipitation over the Indian peninsula during the MWP. The remarkable decreases from the MWP to the LIA are also observed in the retrieved precipitation data from stalagmite records in central India (Sinha et al., 2011). However, another rainfall record in northeastern India (Sinha et al., 2011) shows the opposite trend between the MWP

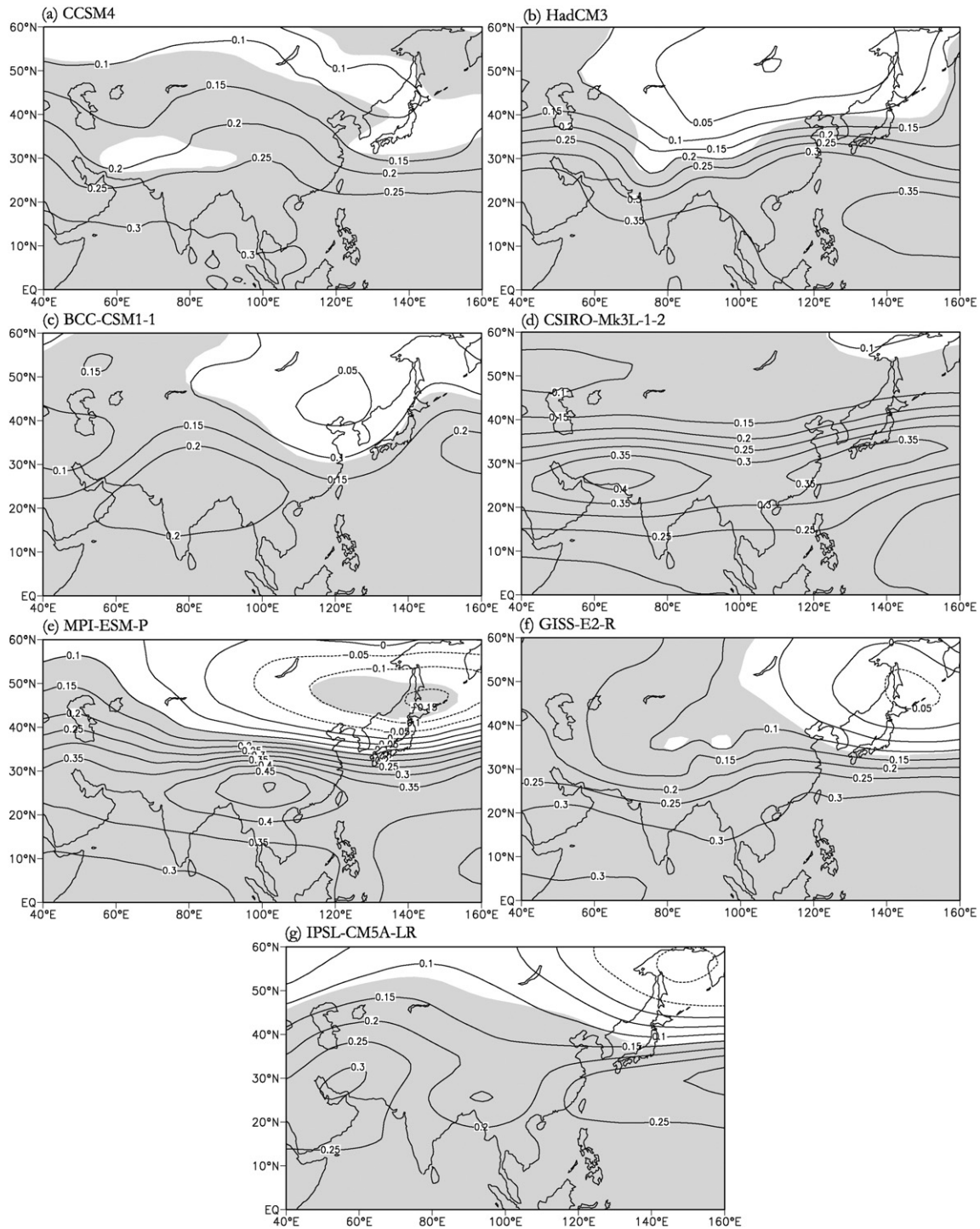


Fig. 11. Differences in the mean temperatures at 200–500 hPa level, between the MWP and LIA. Shaded areas show the regions that are statistically significant at the 95% confidence level.

and LIA, highlighting that there were regional differences in the response of the Indian monsoon.

Resulted from the intensification of the summer monsoon, the simulated precipitation levels over East Asia are similar among most of the models, in that larger precipitation rates occurred during the MWP for the whole of eastern China. A synthesized precipitation record, derived from the stalagmite data and historical documents Tan et al. (2011), proposed a warm-humid/cool-dry pattern in northern central China over the past 1800 years. The MWP was generally accompanied by more rainfall, whereas the LIA was characterized by droughts. Zhang et al. (2008) also suggested that the East

Asian monsoon was stronger, and so the precipitation was heavier, over northern China during the MWP than that in the LIA. These proxy data indicate a wetter climate during the MWP in northern China, which is qualitatively consistent with the model-ensemble results. In contrast, another reconstructed record presents a different rainfall pattern of variation over eastern China; in particular, droughts dominated over the south of the Yangtze River during the ninth to twelfth centuries and then from the middle of the thirteenth century the region was subject to flooding (Zheng et al., 2006). In one of our model simulations (CCSM4), which employs a relatively high resolution, the larger precipitation levels during the MWP do not

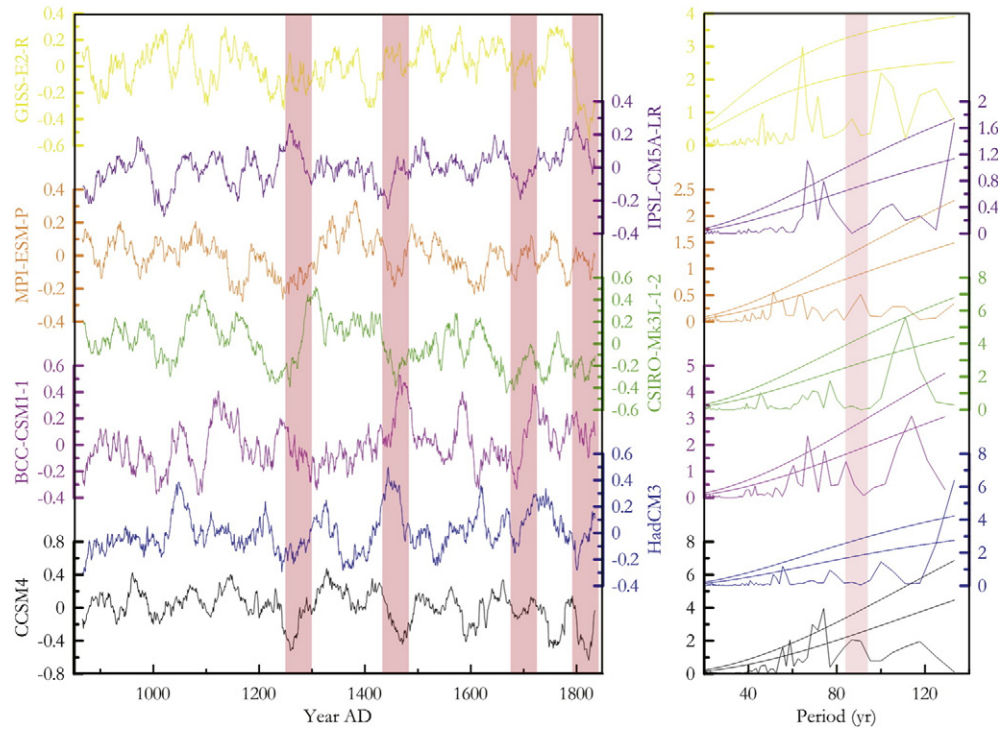


Fig. 12. Simulated 31 year averaged South Asian summer precipitation rates (mm/d, left panel) and their periods (year, right panel) during the past millennium. Pink shading indicates the periods of minimal radiative forcings and the 88 year solar cycles in the left and right panels, respectively. T-test curves used for the 95% and 99% confidence levels are also shown for reference.

occur over eastern China and the change in summer rainfall reverses in the Yangtze River valley, implying a drier MWP in this region.

In contrast to the monsoonal areas, precipitation in the arid central Asia, follows the opposite pattern at the centennial-scale, possibly led by changes in the westerly jet stream. A synthesized moisture curve for central Asia, which covers the past millennium, indicates that a relatively dry condition lasted in the MWP from the eleventh to the thirteenth centuries, and then the moisture increased to high precipitation levels during the LIA (Chen et al., 2010). The models fail to simulate the negative rainfall anomalies during the MWP, compared to the LIA, despite the fact that in most of them the westerly jet in Asia is strengthened. Significant precipitation differences over central Asia as a whole are only detected in two models; the MWP minus the LIA anomaly in one model is negative but in the other it is positive. Thus, the model ensemble does not support the distinct climatic patterns between central Asia and the monsoonal areas in Asia.

4.2. Sensitivity to external forcings

In the multi-model analysis, the simulated NH temperatures are consistently found to be sensitive to the external radiative forcings. Significant annual temperature differences between the MWP and LIA are found among the model simulations, although the sensitivity coefficients are different (the smallest is 0.38 °C·m²/W, in BCC-CSM1-1 and the largest is 1.40 °C·m²/W, in CCSM4). These externally-forced

temperature variations during the last millennium are in agreement with previous studies (Bertrand et al., 2002; Ammann et al., 2007). The Asian monsoon and westerly winds, which are directly controlled by the changes in temperature, respond to the differences in radiative forcing. Most models capture a stronger summer monsoon wind and westerly jet during the MWP, than the LIA, although the regions where their differences are statistically significant are not the same; this sensitivity of the circulations to changes in radiation have previously been simulated (Liu et al., 2011; Man et al., 2012). It is also important to consider the distinct responses between the Asian summer and winter monsoon circulations in the model simulations. In contrast to the simulated stronger summer monsoon during the MWP in most models, the change in the winter monsoon is not consistent; this implies that the warmer conditions prefer a stronger summer monsoon, but the colder conditions do not prefer a stronger winter monsoon, at least in the models.

The models do not capture a significant response of Asian monsoon precipitation to radiative forcing. This simulated weak response of the East Asian summer precipitation is distinctly different from other numerical experiments, which have suggested that the solar and volcanic activities are the dominated forcings for the East Asian monsoon (Liu et al., 2011; Man et al., 2012). In these two studies, remarkable differences were simulated between the MWP and the LIA, or obvious decreases occurred during the minima of radiative forcing. This disagreement, between previous studies and the present one, may be a result of different forcings in the experiments or different definitions of the MWP and LIA. In Liu et al. (2011), the solar irradiation chosen to force their model was several times larger than that preferred by the PMIP3 framework, and of the two, the latter are thought to be more realistic. Thus, our results show that when the radiative forcing is not as strong, it is unable to drive a significant response of Asian monsoon precipitation. The periods of the MWP and LIA in Liu et al. (2011) and Man et al. (2012) only cover 100 years, which is much shorter than this study; the shorter periods may overestimate the contributions from external forcing, because the internal oscillations within the

Table 4
Differences in Asian precipitation rates (mm/d) between the Medieval Warm Period and the Little Ice Age. **/* indicates statistically significant differences at 99%/95% levels, respectively.

	CCSM	HadCM	BCC	CSIRO	MPI	GISS	IPSL
South Asian Pr	0.16*	-0.06	0.05	0.21**	0.05	0.02	-0.06
East Asian Pr	0.04	0.11*	-0.08	0.07	0.10**	0.12**	0.09*
Central Asian Pr	0.01	0.0	0.02*	-0.02**	0.01	0.0	0.0

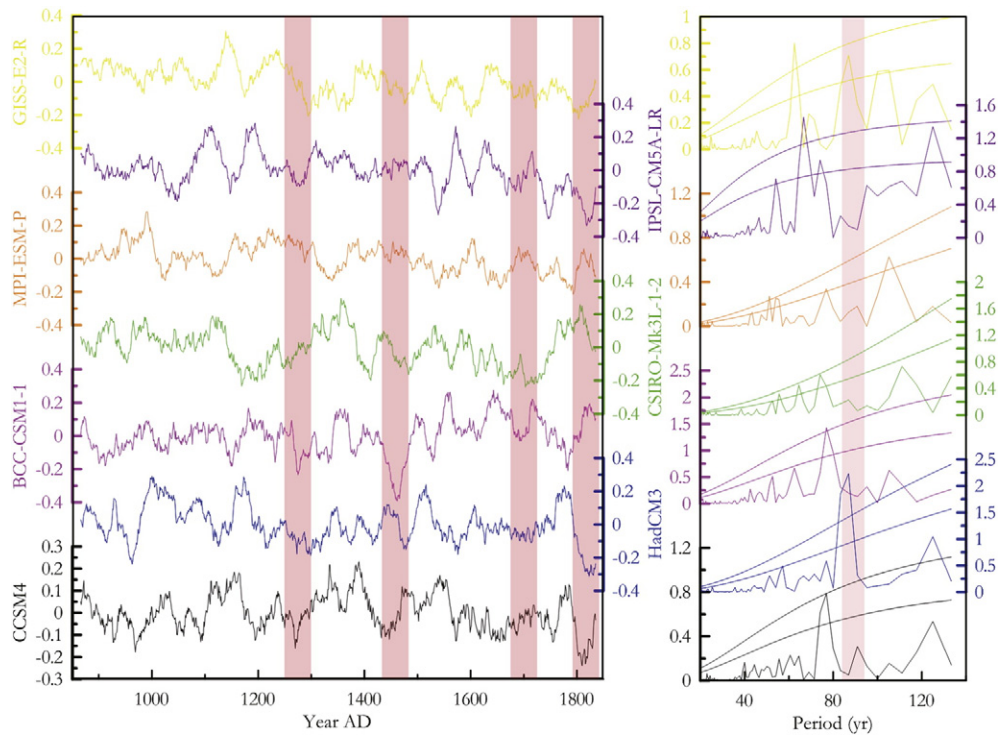


Fig. 13. Simulated 31 year averaged East Asian summer precipitation rates (mm/d, left panel) and their periods (year, right panel) during the past millennium. Pink shading indicates the periods of minimal radiative forcings and the 88 year solar cycles in the left and right panels, respectively. T-test curves used for the 95% and 99% confidence levels are also shown for reference.

climate system (e.g., Atlantic Multi-decadal Oscillation) can also affect the Asian monsoon on the multi-decadal to centennial timescales.

In addition to the amplitude, the forced mode of the East Asian summer precipitation is also different among the models. Five of the models in our study simulate increases in the summer precipitation over

eastern China (Fig. 11), which is consistent with Liu et al. (2011). This forced mode of the East Asian precipitation is distinct from the observed multi-polar pattern on the interannual timescale and the so-called “south-flood–north-drought” pattern that occurs on the decadal timescale. In contrast, a tripolar pattern of the summer precipitation is

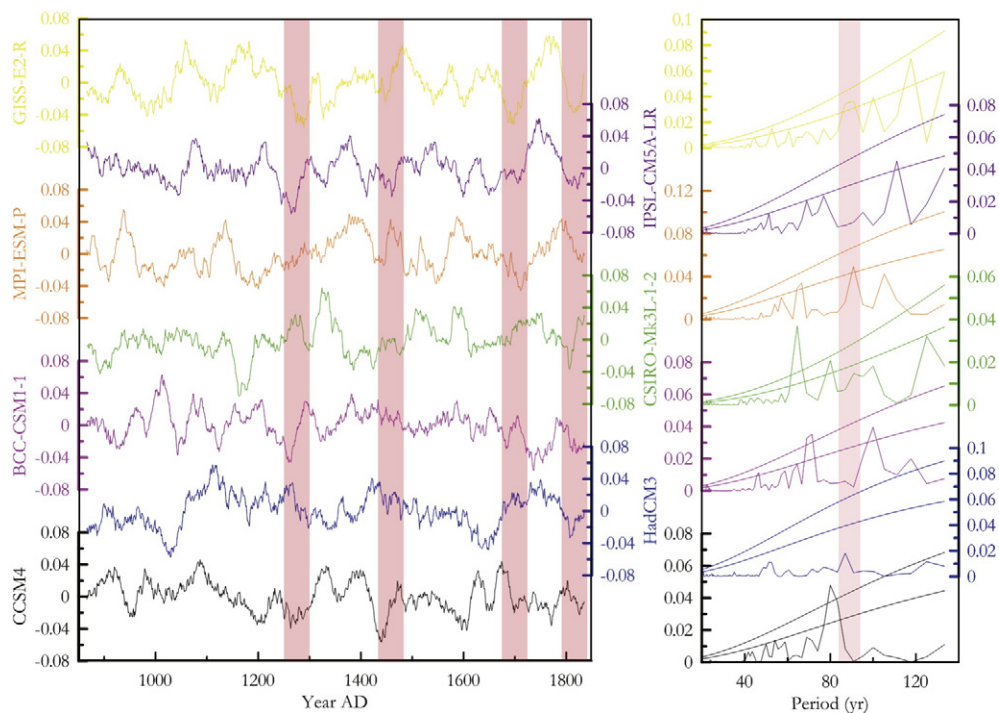


Fig. 14. Simulated 31 year averaged Central Asian annual precipitation rates (mm/d, left panel) and their periods (year, right panel) during the past millennium. Pink shading indicates the periods of minimal radiative forcings and the 88 year solar cycles in the left and right panels, respectively. T-test curves for the 95% and 99% confidence levels are also shown for reference.

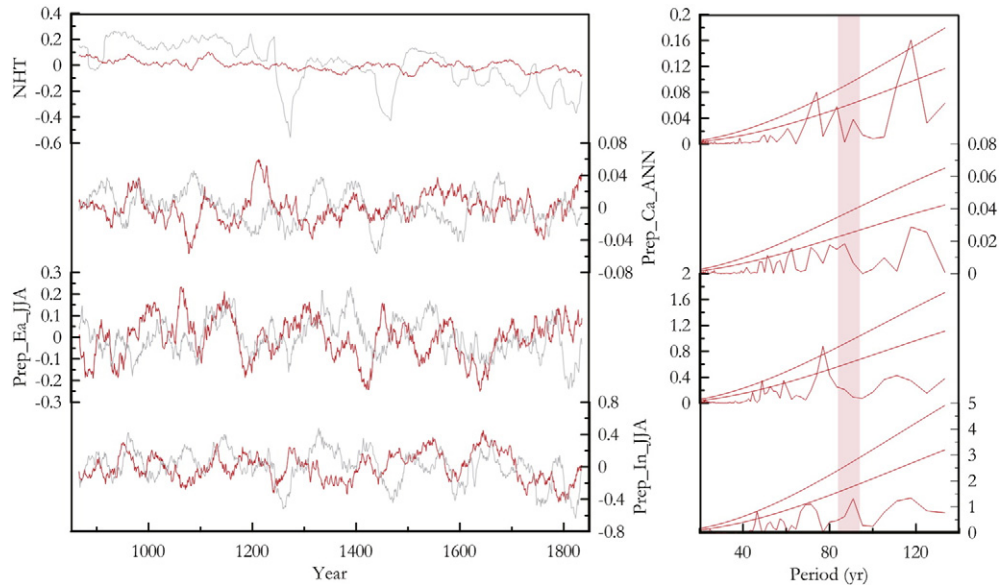


Fig. 15. Simulated 31 year averaged northern hemisphere surface temperature and Asian precipitation rates in the CCSM4 control run (mm/d, pink, left panel) and their periods (year, right panel) during the past millennium. T-test curves used for the 95% and 99% confidence levels are also shown for reference. The corresponding values (gray) for the CCSM4 LM run are also shown for comparison.

simulated in CCSM4, which is characterized by a negative anomaly over the Yangtze River valley and two positive anomalies over tropical and northern China. This feature is consistent with the results of Man et al. (2012), although the simulated responses of the circulation are not the same. Thus, the variations in East Asian rainfall during the last millennium are highly model-dependent; the discrepancies among the models might originate from the different spatial resolutions and the model performances. Anyhow, our results indicate that the Asian monsoon rainfall is not substantially influenced by external forcings, which is different from the findings of previous studies that have used both modeling and proxy data (Agnihotri et al., 2002; Zhang et al., 2008; Tan et al., 2011; Liu et al., 2011; Man et al., 2012).

5. Conclusions

Using the outputs from last millennium (A.D. 850–1850) experiments by seven coupled ocean–atmosphere models, the variations of Asian climate and the differences between the MWP and LIA have been analyzed, in order to evaluate the effect of solar irradiation and volcanic forcing. The surface temperatures over Asia, similar to the temperature changes at the hemispheric-scale, undergo a remarkable change from the MWP to the LIA, as a direct response to the weakening of radiative forcing that occurs during this period. Following changes in the thermal structure, the intensified ocean–land contrast in temperatures during summer lead to stronger Asian summer monsoon winds in the MWP, compared to the LIA. Significant anomalies also occur in changes to the Asian westerly jet during winter. These consistent features in the different models indicate that the variations of temperature and associated circulations during the last millennium, are forced responses to the external radiative forcing.

During the modeling years, strong multi-decadal to centennial variations also occur in the Asian monsoon precipitation; however, these variations are strongly model-dependent. Although some differences between the MWP and LIA are captured in certain models, nearly all of the models fail to simulate the weaker-radiation–less-rainfall relationship, for both the East and south Asia regions. Thus, it is concluded that the monsoon-associated precipitation is not sensitive to the external radiation changes and more likely a result of internal oscillations. The question of whether, and how, the solar irradiation and volcanic forcings affect the Asian climate needs further, extensive researches.

By gaining a comprehensive knowledge of the variability and mechanisms behind the Asian climate during the last millennium, we would be able to provide authentic constraints for future climate change.

Acknowledgments

The authors thank Dr. Bette Otto-Bliesner for her help in accessing the modeling data and writing this manuscript. This work was jointly supported by the National Basic Research Program of China (2013CB955904), the Key Research Program of Chinese Academy of Sciences (KZZD-EW-04-07) and the National Natural Science Foundation of China (41290255, 41572160).

References

- Agnihotri, R., Dutta, K., Bhushan, R., Somayajulu, B.L.K., 2002. Evidence for solar forcing on the Indian monsoon during the last millennium. *Earth Planet. Sci. Lett.* 198, 521–527.
- Ammann, C.M., Joos, F., Schimel, D.S., Otto-Bliesner, B.L., Tomas, R.A., 2007. Solar influence on climate during the past millennium: results from transient simulations with the NCAR climate system model. *Proc. Natl. Acad. Sci. U. S. A.* 104, 3713–3718.
- An, Z.S., et al., 2012. Interplay between the westerlies and Asian monsoon recorded in Lake Qinghai sediments since 32 ka. *Sci. Rep.* 2. <http://dx.doi.org/10.1038/srep00619>.
- An, Z.S., Wu, G.X., Li, J.P., Sun, Y.B., Liu, Y.M., Zhou, W.J., Cai, Y.J., Duan, A.M., Li, L., Mao, J.Y., Cheng, H., Shi, Z.G., Tan, L.C., Yan, H., Ao, H., Chang, H., Feng, J., 2015. Global monsoon dynamics and climate change. *Annu. Rev. Earth Planet. Sci.* 43, 2.1–2.49.
- Anderson, D.M., Overpeck, J.T., Gupta, A.K., 2002. Increase in the Asian southwest monsoon during the past four centuries. *Science* 297, 596–599.
- Berkehamer, M., Sinha, A., Mudelsee, M., Cheng, H., Edwards, R.L., Cannariato, K., 2010. Persistent multidecadal power of the Indian summer monsoon. *Earth Planet. Sci. Lett.* 290, 166–172.
- Bertrand, C., Loutre, M., Crucifix, M., Berger, A., 2002. Climate of the last millennium: a sensitivity study. *Tellus A* 54, 3221–3244.
- Brovkin, V., Ganopolski, A., Claussen, M., Kubatzki, C., Petoukhov, V., 1999. Modelling climate response to historical land cover change. *Glob. Ecol. Biogeogr.* 8, 509–517.
- Chang, C.P., Harr, P., Ju, J., 2001. Possible roles of Atlantic circulations on the weakening Indian monsoon rainfall-ENSO relationship. *J. Clim.* 14, 2376–2380.
- Chen, F.H., Yu, Z., Yang, M., Ito, E., Wang, S., Madsen, D.B., Huang, X., Zhao, Y., Sato, T., Birks, J.B., Boomer, I., Chen, J., An, C., 2008. Holocene moisture evolution in arid central Asia and its out-of-phase relationship with Asian monsoon history. *Quat. Sci. Rev.* 27, 351–364.
- Chen, F.H., Chen, J.H., Holmes, J., Boomer, I., Austin, P., Gates, J.B., Wang, N.L., Brooks, S.J., Zhang, J.W., 2010. Moisture changes over the last millennium in arid central Asia: a review, synthesis and comparison with monsoon region. *Quat. Sci. Rev.* 29, 1055–1068.
- Cook, E.R., Anchukaitis, K.J., Buckley, B.M., D'Arrigo, R.D., Jacoby, G.C., Wright, W.E., 2010. Asian monsoon failure and megadrought during the last millennium. *Science* 328, 486–489.

- Crowley, T.J., Zielinski, G., Vinther, B., Udisti, R., Kreutz, K., Cole-Dai, J., Castellano, E., 2008. Volcanism and the Little Ice Age. *PAGES Newslett.* 16, 22–23.
- Ding, Y., Chan, J.C., 2005. The East Asian summer monsoon: an overview. *Meteorol. Atmos. Phys.* 89, 117–142.
- Fan, F., Mann, M.E., Ammann, C.M., 2009. Understanding changes in the Asian summer monsoon over the past millennium: insights from a long-term coupled model simulation. *J. Clim.* 22, 1736–1748.
- Gadgil, S., 2003. The Indian monsoon and its variability. *Annu. Rev. Earth Planet. Sci.* 31, 429–467.
- Gao, C.C., Robock, A., Ammann, C., 2008. Volcanic forcing of climate over the past 1500 years: an improved ice core-based index for climate models. *J. Geophys. Res.* 113, D23111. <http://dx.doi.org/10.1029/2008JD010239>.
- Goosse, H., Renssen, H., Timmermann, A., Bradley, R.S., 2005. Internal and forced climate variability during the last millennium: a model-data comparison using ensemble simulations. *Quat. Sci. Rev.* 24, 1345–1360.
- Goswami, B.N., Xavier, P.K., 2005. ENSO control on the south Asian monsoon through the length of the rainy season. *Geophys. Res. Lett.* 32. <http://dx.doi.org/10.1029/2005GL023216>.
- Goswami, B.N., Madhusoodanan, M.S., Neema, C.P., Sengupta, D., 2006. A physical mechanism for North Atlantic SST influence on the Indian summer monsoon. *Geophys. Res. Lett.* 33. <http://dx.doi.org/10.1029/2005GL024803>.
- Graham, N.E., Ammann, C.M., Fleitmann, D., Cobb, K.M., Luterbacher, J., 2011. Support for global climate reorganization during the “Medieval Climate Anomaly”. *Clim. Dyn.* 37, 1217–1245.
- Krishnamurti, V., Goswami, B.N., 2000. Indian monsoon–ENSO relationship on interdecadal timescale. *J. Clim.* 13, 579–595.
- Kumar, K.K., Rajagopalan, B., Cane, M.A., 1999. On the weakening relationship between the Indian monsoon and ENSO. *Science* 284, 2156–2159.
- Li, J., Wu, Z., Jiang, Z., He, J., 2010. Can global warming strengthen the East Asian summer monsoon? *J. Clim.* 23, 6696–6705.
- Liu, J., Wang, B., Wang, H., Kuang, X., Ti, R., 2011. Forced response of the East Asian summer rainfall over the past millennium: results from a coupled model simulation. *Clim. Dyn.* 36, 323–336.
- Lu, R., Ye, H., Jhun, J., 2011. Weakening of interannual variability in the summer East Asian upper-tropospheric westerly jet since the mid-1990s. *Adv. Atmos. Sci.* 28, 1246–1258.
- Man, W., Zhou, T., Jungclaus, J.H., 2012. Simulation of the East Asian summer monsoon during the last millennium with the MPI earth system model. *J. Clim.* 25, 7852–7866.
- Newton, A., Thunell, R., Stott, L., 2006. Climate and hydrographic variability in the Indo-Pacific warm pool during the last millennium. *Geophys. Res. Lett.* 19. <http://dx.doi.org/10.1029/2006GL027234>.
- Qian, W., Hu, Q., Zhu, Y., Lee, D.K., 2003. Centennial-scale dry-wet variations in East Asia. *Clim. Dyn.* 21, 77–89.
- Rajagopalan, B., Molnar, P., 2012. Pacific Ocean sea-surface temperature variability and predictability of rainfall in the early and late parts of the Indian summer monsoon season. *Clim. Dyn.* 39, 1543–1557.
- Schmidt, G.A., et al., 2012. Climate forcing reconstructions for use in PMIP simulations of the last millennium (v1.1). *Geosci. Model Dev.* 5, 185–191.
- Shapiro, A.I., Schmutz, W., Rozanov, E., Schoell, M., Haberleiter, M., Shapiro, A.V., Nyeki, S., 2011. A new approach to the long-term reconstruction of the solar irradiance leads to large historical solar forcing. *Astron. Astrophys.* 529, A67. <http://dx.doi.org/10.1051/0004-6361/201016173>.
- Shen, C., Wang, W.C., Peng, Y., Xu, Y., Zheng, J., 2008. Variability of summer precipitation over eastern China during the last millennium. *Clim. Past* 5, 129–141.
- Shi, Z., Yan, X., Yin, C., Wang, Z., 2007. Effects of historical land cover changes on climate. *Chin. Sci. Bull.* 52, 2575–2583.
- Shi, Z., Liu, X., Liu, Y., Sha, Y., Xu, T., 2014. Impact of Mongolian Plateau versus Tibetan Plateau on the westerly jet over North Pacific Ocean. *Clim. Dyn.* <http://dx.doi.org/10.1007/s00382-014-2217-2>.
- Sinha, A., Cannariato, K.G., Stott, L.D., Cheng, H., Edwards, R.L., Yadava, M.G., Ramesh, R., Singh, I.B., 2007. A 900-yr (600 to 1500 A.D.) record of the Indian summer monsoon precipitation from the core monsoon zone of India. *Geophys. Res. Lett.* 34. <http://dx.doi.org/10.1029/2007GL030431>.
- Sinha, A., Stott, L., Berkelhammer, M., Cheng, H., Edwards, R.L., Buckley, B., Aldenderfer, M., Mudelsee, M., 2011. A global context for megadroughts in monsoon Asia during the past millennium. *Quat. Sci. Rev.* 30, 47–62.
- Sinha, A., Kathayat, G., Cheng, H., Breitenbach, S., Berkelhammer, M., Mudelsee, M., Biswas, J., Edwards, R.L., 2015. Trends and oscillations in the Indian summer monsoon rainfall over the last two millennia. *Nat. Commun.* 6. <http://dx.doi.org/10.1038/ncomms7309>.
- Sooraj, K.P., Terray, P., Mujumdar, M., 2014. Global warming and the weakening of the Asian summer monsoon circulation: assessments from the CMIP5 models. *Clim. Dyn.* <http://dx.doi.org/10.1007/s00382-014-2257-7>.
- Steinhilber, F., Beer, J., Fröhlich, C., 2009. Total solar irradiance during the Holocene. *Geophys. Res. Lett.* 36, L19704. <http://dx.doi.org/10.1029/2009GL040142>.
- Sun, J., Wang, H., Yuan, W., 2008. A possible mechanism for the co-variability of the boreal spring Antarctic oscillation and the Yangtze River valley summer rainfall. *Int. J. Climatol.* <http://dx.doi.org/10.1002/joc.1773>.
- Tan, L., Cai, Y., An, Z., Yi, L., Zhang, H., Qin, S., 2011. Climate patterns in north central China during the last 1800 yr and their possible driving force. *Clim. Past* 7, 685–692.
- Ueda, H., Iwai, A., Kuwako, K., Hori, M.E., 2006. Impact of anthropogenic forcing on the Asian summer monsoon as simulated by eight GCMs. *Geophys. Res. Lett.* <http://dx.doi.org/10.1029/2005GL025336>.
- Ummerhofer, C., Gupta, A., Li, Y., Taschetto, A., England, M., 2011. Multi-decadal modulation of the El Niño–Indian monsoon relationship by Indian Ocean variability. *Environ. Res. Lett.* 6. <http://dx.doi.org/10.1088/1748-9326/6/3/034006>.
- Verschuren, D., Laird, K., Cumming, B., 2000. Rainfall and drought in east Africa during the past 1100 years. *Nature* 403, 410–414.
- Vieira, L.E.A., Solanki, S.K., Krivova, N.A., Usoskin, I., 2011. Evolution of the solar irradiance during the Holocene. *Astron. Astrophys.* 531, A6. <http://dx.doi.org/10.1051/0004-6361/201015843>.
- von Rad, U., Schaaf, M., Michels, K.H., Schulz, H., Berger, W.H., Sirocko, F., 1999. A 5000-yr record of climate change in varved sediments from the oxygen minimum zone off Pakistan, northeastern Arabian sea. *Quat. Res.* 51, 39–53.
- Wang, B., 2006. *The Asian Monsoon*. Springer/Praxis Publishing, New York, p. 787.
- Wang, Y., Cheng, H., Edwards, R.L., He, Y., Kong, X., An, Z., Wu, J., Kelly, M.J., Dykosk, C.A., Li, X., 2005. The Holocene Asian monsoon: links to solar changes and North Atlantic climate. *Science* 308, 854–857.
- Wang, S., Wen, X., Luo, Y., Dong, W., Zhao, Z., Yang, B., 2007. Reconstruction of temperature series of China for the last years. *Chin. Sci. Bull.* 52, 3272–3280.
- Wang, B., Yang, J., Zhou, T., 2008. Interdecadal changes in the major modes of Asian–Australian monsoon variability: strengthening relationship with ENSO since the late 1970s. *J. Clim.* 21, 1771–1789.
- Wu, R., Wang, B., 2002. A contrast of the East Asian summer monsoon–ENSO relationship between 1962 and 77 and 1978–93. *J. Clim.* 15, 3266–3279.
- Xu, T., Shi, Z., Wang, H., An, Z., 2015. Nonstationary impact of the winter north Atlantic oscillation and the response of mid-latitude Eurasian climate. *Theor. Appl. Climatol.* <http://dx.doi.org/10.1007/s00704-015-1396-z>.
- Yang, B., Braeuning, A., Johnson, K.R., Shi, Y.F., 2002. General characteristics of temperature variation in China during the last two millennia. *Geophys. Res. Lett.* <http://dx.doi.org/10.1029/2001GL014485>.
- Zhang, Y., Kuang, X., Guo, W., Zhou, T., 2006. Seasonal evolution of the upper-tropospheric westerly jet core over East Asia. *Geophys. Res. Lett.* 33. <http://dx.doi.org/10.1029/2006GL026377>.
- Zhang, P., et al., 2008. A test of climate, sun and culture relationships from an 1810-year Chinese cave record. *Science* 322, 940–942.
- Zheng, J., Wang, W., Ge, Q., Man, Z., Zhang, P., 2006. Precipitation variability and extreme events in eastern China during the past 1500 years. *Terr. Atmos. Ocean. Sci.* 17, 579–592.
- Zhou, T., Gong, D., Li, J., Li, B., 2009. Detecting and understanding the multi-decadal variability of the East Asian summer monsoon – recent progress and state of affairs. *Meteorol. Z.* 18, 455–467.
- Zorita, E., von Storch, H., Gonzalez-Rouco, F.J., Cubasch, U., Luterbacher, J., Legutke, S., Fischer-Bruns, I., Schlese, U., 2004. Climate evolution in the last five centuries simulated by an atmosphere–ocean model: global temperatures, the North Atlantic oscillation and the late Maunder minimum. *Meteorol. Z.* 13, 271–289.